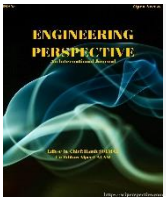

e-ISSN:2757-9077

ENGINEERING PERSPECTIVE

https://sciperspective.com/ Research Paper

Magnetocaloric Cooling for Hybrid/Hydrogen and Electric Vehicle Cabin and Powertrain Components

Mohand Ouyahia Bousseksou[1*], Kamal Nouri[1], Thomas Bartoli[1], Wassim Bouzidi[1], Lotfi Bessais[2]

[1]*Capgemini engineering, Ile de France, Division APA, 12 rue de la Verrerie, 92190 Meudon, France*
[2]*CNRS-UPEC, Université Paris Est, ICMPE (UMR 7182), F-94320 Thiais, France*

ABSTRACT

The magnetocaloric cooling system is a promising alternative to traditional refrigeration systems that rely on the compression and expansion of harmful refrigerant gases. Utilizing the magnetocaloric effect, these systems can efficiently provide heating and cooling for a wide range of applications. One particularly significant application of this technology is in the air conditioning of electric vehicles and the thermal management of powertrain components.

This study presents a Matlab Simulink model of the powertrain, alongside a COMSOL model of the permanent magnet, specifically designed for hybrid and electric car applications. The Matlab Simulink model simulates the dynamic behavior of the vehicle's powertrain, integrating the magnetocaloric cooling system to analyze its impact on performance and efficiency. This allows for a comprehensive evaluation of how the system can improve energy efficiency and thermal regulation in electric vehicles. Additionally, the COMSOL model focuses on the detailed behavior of the permanent magnet used in the magnetocaloric cooling system. This model provides insights into the magnetic field distribution and its interaction with the magnetocaloric materials, which are critical for optimizing the cooling cycle and enhancing overall system performance.

To ensure the accuracy and reliability of the simulations, some interpolated experimental data were used. This data helps in refining the models, ensuring that they closely represent real-world scenarios and behaviors. By combining these advanced modeling techniques, the study aims to demonstrate the feasibility and benefits of implementing magnetocaloric cooling systems in electric and hybrid vehicles, potentially leading to more sustainable and efficient automotive thermal management solutions.

Keywords: Magnetocaloric; Cooling system; Matlab Simulink; COMSOL; Automotive.

History
Received: 31.07.2024
Accepted: 16.12.2024

Author Contacts
*Corresponding Author
e-mail addresses : mohand-ouyahia.bousseksou@capgemini.com

How to cite this paper: Bousseksou, M.O., Nouri, K., Bartoli, T., Bouzidi, W., Bessais, L., (2025). Magnetocaloric Cooling for Hybrid/ Hydrogen and Electric Vehicle Cabin and Powertrain Components. Engineering Perspective, 5 (1), 9-20. http://dx.doi.org/10.29228/eng.pers.77695

1. Introduction

The automotive industry is facing a technological revolution to achieve high global environmental goals. The use of new drive concepts such as pure electric or hybrid drives is a considerable success factor for more sustainable transportation. In a vehicle with these new concepts, the hybrid or 100% electric powertrain is of great technological importance [1].

The hybrid powertrain is made up of three components: the combustion engine, the electric motor powered by an energy storage system (such as a battery or fuel cell) and the power electronics that generate heat and require cooling. Several techniques have been implemented to recover heat sources and optimize energy harvesting. The development of innovative materials explored is to ensure and optimize the thermal management of all the organs of the hybrid powertrain of vehicles. The selection of magnetocaloric materials depends on the desired application. Taking gadolinium [2] as an example, to have a significant magnetocaloric effect (MCE), a temperature range of about 25 K before and after the curie transition (CT) is required. For the automotive sector, the range is 270 K to 340 K under a magnetic field of 0-1.5 T. Gd-based alloys may therefore be an ideal colling choice for various vehicle components.

Today, magnetic cooling has attracted considerable interest in scientific research, and many prototypes have been built by laboratories and companies such as Toshiba, Toyota, Astronautics, or even COOLTECH Applications [3] [4]. Magnetic cooling is

based on the MCE, which results in the heating of a material following its magnetization, also in its cooling during its demagnetization [5][6][7][8]. In the case of conventional refrigeration, a gas is used that undergoes cycles of compression / expansion. To put it another way, heating, or cooling. An equivalent principle is applied for magnetic cooling; it is a system in which a material with a magnetocaloric effect is subjected to a magnetization and demagnetization cycle. New multifunctional materials for magnetic cooling are produced that possess great magnetocaloric effects, such as compounds like gadolinium (Gd), manganese (Mn), oxides, intermetallic [9][10][11]perovskites, ceramics... etc. For applications below 270 K, other materials must be used. Pecharsky and Jr. Gschneidner [12] discovered a "giant" magnetocaloric effect in the alloy (Gd5(Si2Ge2)). Based on these studies, scientists and the refrigeration industry are beginning to seriously consider magnetic cooling at room temperature for industrial applications. There are also other materials with a giant magnetocaloric effect, such as MnAs1-xSbx [13], La(Fe1-xSix)13 [14]or MnFePxAs1-x [15].

This ecological process could ensure the cooling of the different components of the hybrid-electric powertrain. This new approach will reduce vehicle weight, fuel consumption, increase vehicle range, and improve environmental impact. This paper develops a new technology to efficiently cool the hybrid-electric powertrain.

The aim of this work is to develop a 1D model on MATLAB and a 2D model on COMSOL. These modelling were conducted to study the magnetocaloric effect and the cooling power to efficiently cool the hybrid-electric powertrain and the cabin.

2. Thermodynamic approach and simulation equations

In this section, the thermodynamic approach of the magnetocaloric effect has been developed, as well as the equations necessary for the theoretical modelling and numerical simulations of the magnetic cooling system. A thermodynamic system can be described in terms of variables states. There are two types: extensive, which depend on the size of the system studied, and intensive, which do not. The entropy of a magnetic material at constant pressure depends on the applied magnetic field H and the temperature T. It is defined as the sum of the contributions of the entropies, magnetic ($S_M(T,H)_P$), lattice ($S_R(T)_P$) and electronic ($S_E(T)_P$):

$$\boldsymbol{S(T,H) = S_M(T,H)_P + S_R(T)_P + S_E(T)_P} \quad (1)$$

The thermodynamic properties of a system, where T and P are fixed, and described by the Gibbs free energy G. The magnetic system is defined at constant pressure as a function of the temperature T, the pressure P, and the applied field H:

$$\boldsymbol{G(P,H,T) = U + PV - TS - \mu_0 MH} \quad (2)$$

Where μ_0 is the magnetic permeability of the vacuum, U is the internal energy of the system, P, H and T are intensive variables (pressure, magnetic field and temperature) and V, M and S are the extensive variables (volume, magnetization and entropy).

The total differential of G is given by:

$$\boldsymbol{dG(P,H,T) = dU + PdV + VdP - TdS - SdT - \mu_0 MdH - \mu_0 HdM} \quad (3)$$

On the other hand, we can write:

$$\boldsymbol{dG(P,H,T) = \left(\frac{\partial G}{\partial P}\right)_{T,H} dP + \left(\frac{\partial G}{\partial T}\right)_{P,H} dT + \left(\frac{\partial G}{\partial H}\right)_{P,T} dH} \quad (4)$$

By identifying the two equations (3) and (4), the variation of the internal energy is written:

$$\boldsymbol{dU = TdS + \mu_0 HdM + PdV} \quad (5)$$

Therefore, dG reduces to:

$$dG(P,H,T) = VdP - \mu_0 MdH - SdT \quad (6)$$

Using equations (4) and (6), we have:

$$\boldsymbol{V = \left(\frac{\partial G}{\partial P}\right)_{T,H}} \quad (7)$$

$$\boldsymbol{\mu_0 M = -\left(\frac{\partial G}{\partial H}\right)_{P,T}} \quad (8)$$

$$\boldsymbol{S = -\left(\frac{\partial G}{\partial T}\right)_{P,H}} \quad (9)$$

By deriving equations (7) and (8), we obtain Maxwell's relation [16]:

$$\mu_0\left(\frac{\partial M}{\partial T}\right) = -\left(\frac{\partial}{\partial T}\right)\left(\frac{\partial G}{\partial H}\right) = -\left(\frac{\partial}{\partial H}\right)\left(\frac{\partial G}{\partial T}\right) = \left(\frac{\partial S}{\partial H}\right) \quad (10)$$

Therefore,

$$\mu_0\left(\frac{\partial G}{\partial T}\right)_{P,H} = \left(\frac{\partial S}{\partial H}\right)_{P,T} \quad (11)$$

3. Thermodynamic approach and simulation equations

To determine the variation of the maximum magnetic entropy, we integrate the previously established relationship between two magnetic field values, assuming an isothermal transformation:

$$\int_{H1}^{H2} \mu_0\left(\frac{\partial M}{\partial T}\right)_{P,H} dH = \int_{H1}^{H2} \left(\frac{\partial S}{\partial H}\right)_{P,T} dH = \Delta S(T,\Delta H) \quad (12)$$

This entropy variation is noted as magnetic entropy variation since we assumed from the beginning that the application of a magnetic field affects only the magnetic order, and we can therefore write:

$$\int_{H1}^{H2} \mu_0\left(\frac{\partial M}{\partial T}\right)_{P,H} dH = \Delta S_M(T,\Delta H) \quad (13)$$

Equation (12) shows that the change in magnetic entropy Δ (T,

ΔH) is proportional to the derivative of the magnetization with respect to temperature at constant field and the change in the magnetic field. If the field varies between 0 and H, then equation (12) is written:

$$\Delta S_M(T, \Delta H) = \int_0^H \mu_0 \left(\frac{\partial M}{\partial T}\right)_{P,H} dH \quad (14)$$

The variation in magnetic entropy can be determined by integrating the magnetization isotherms. It is important to highlight that based on the measurements of the material's magnetization as a function of temperature M (T) and magnetic field M (H), it is possible to obtain the value of ΔS, at different fields and temperatures, after numerical integration according to the following formula [17]:

$$\Delta S_M(T_i, \Delta H) = \mu_0 \sum_i \frac{M_{i+1} - M_i}{T_{i+1} - T_i} \Delta H_i \quad (15)$$

With:

μ_0: magnetic permeability of the vacuum.

M_i, M_{i+1} : magnetization measured at T_i, T_{i+1} to the variation of the applied field ΔH_i.

We recall that ΔS and RCP are the two main quantities of the magnetocaloric effect (MCE). The value of enables us to characterize magnetocaloric materials by the relative cooling power (RCP). It corresponds to the amount of heat that can be transferred from the hot source to the cold source of a cooling system. It can be described for a given magnetic field by the following relation:

$$RCP = -\Delta S_M^{max} \times \delta T_{FWHM} \quad (16)$$

Or ΔS_M^{max} is the maximum value of the magnetic entropy change and δT_{FWHM} the maximum half-height width of the corresponding ΔS_M.

4. Result and discussions

A 1D model on Matlab-Simulink is used to model the magnetocaloric effect, the cooling of the powertrain components and the driver cabin, and a 2D model on COMSOL is established to determine the characteristics of the permanent magnet.

4.1 Matlab Simulink model

The Simulink model of the cooling system provide the use of a thermodynamic cycle based on the magnetocaloric effect for the cooling of the powertrain and cabin (or even the heating of the cabin if we use the reversibility of the system).

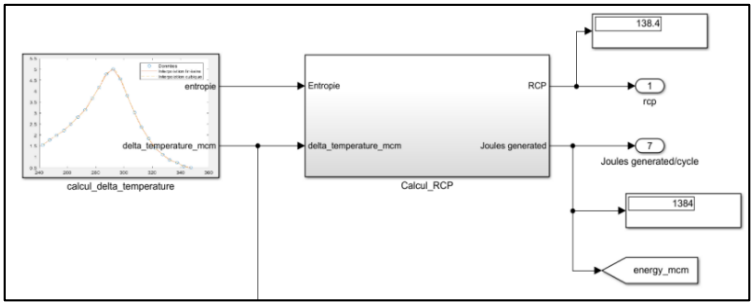

Figure 1. Simulink Block of the MCM and Permanent magnet

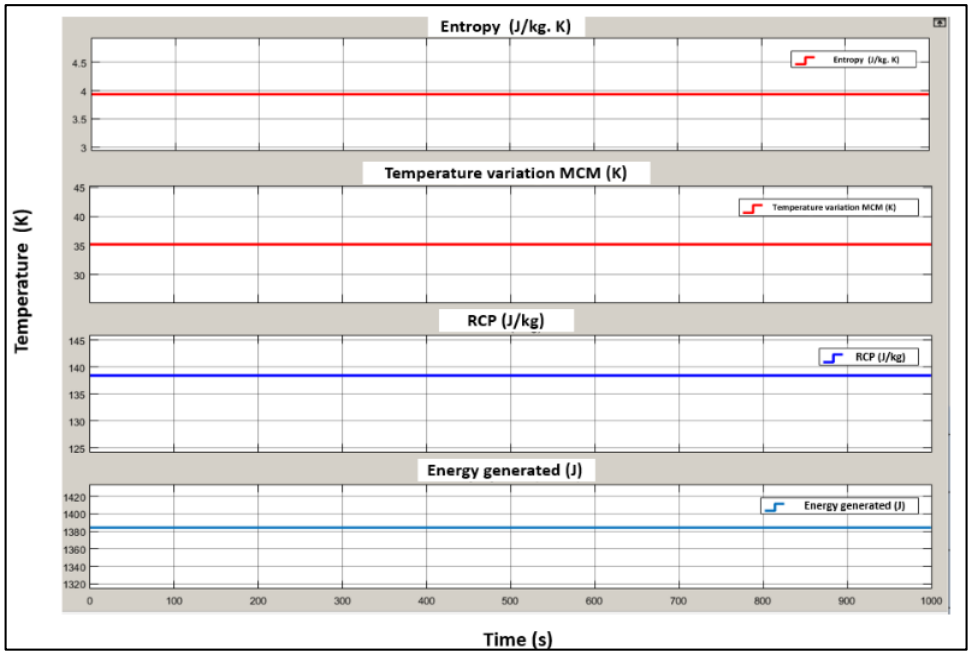

Figure 2. The simulation result vs time of the following parameters: Entropy, temperature variation, Relative cooling power and the energy produced

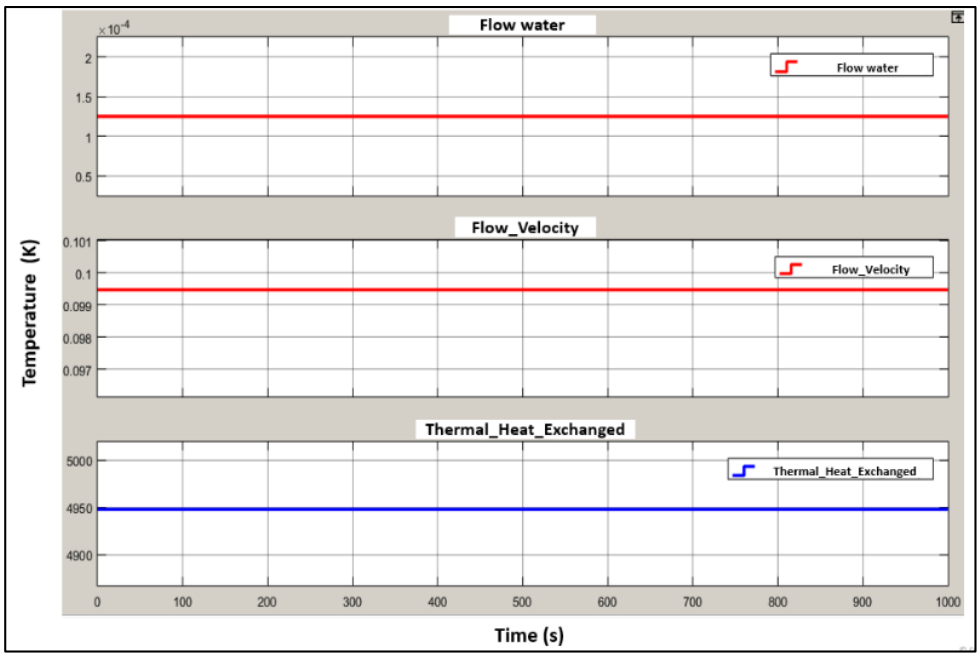

Figure 3. The simulation result vs time of the following parameters: mass flow rate of water, flow velocity and the thermal heat ex-changed

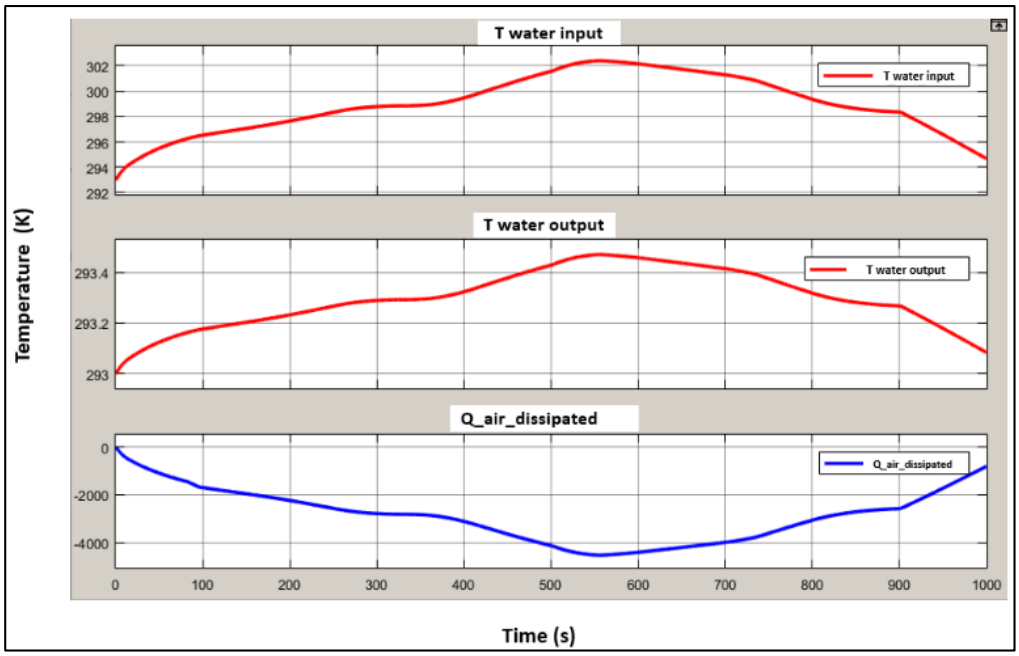

Figure 4. The simulation result vs time of the following parameters: water at radiator inlet, water at radiator outlet and dissipated energy of the air

Part 1: Magnetocaloric material (MCM) & Permanent Magnet block

Using the Matlab script, two magnetic entropy variation maps (0–1 T & 0–2 T) which are averaged to calculate the magnetic entropy ΔS and the temperature variation ΔT at a magnetic field applied of 1.5 T (Figure 1). The Gd is taken as a reference for the magnetocaloric around room temperature. The value of the maximum magnetic entropy of Gd is equal to 3.8 J/kg. K [18]. The relative cooling power (RCP) is calculated as follows:

$$\mathrm{RCP} = \Delta S_{\max} \times \Delta T = 138.5 \ \mathrm{J/kg} \quad (17)$$

The energy generated depends on the mass of magnetocaloric material (MCM) (10 kg for this use case). The energy generated (Figure 2):

$$Q = \mathrm{RCP} \times \mathrm{mass\ of\ MCM} = 1385 \ \mathrm{J} \quad (18)$$

The external convection was used for the calculation of heat transfer, this approximation is used for uniform plates with a laminar regime for the heat transfer fluid (Water). For the convection study, we are used the same thermodynamic simulation cited in this [2].

The energy Q1 transported in the heat transfer fluid (water) is calculated based on the water flow rate and the flow velocity. For a flow rate of 0.000125 m^3/s = 7.5 l/min, this fluid flow generates energy Q1 = 4950 J (Figure 3). This Q1 energy is greater than Q (Q1 > Q), the flow rate of 7.5 l/min is therefore sufficient to absorb the energy generated by the MCM.

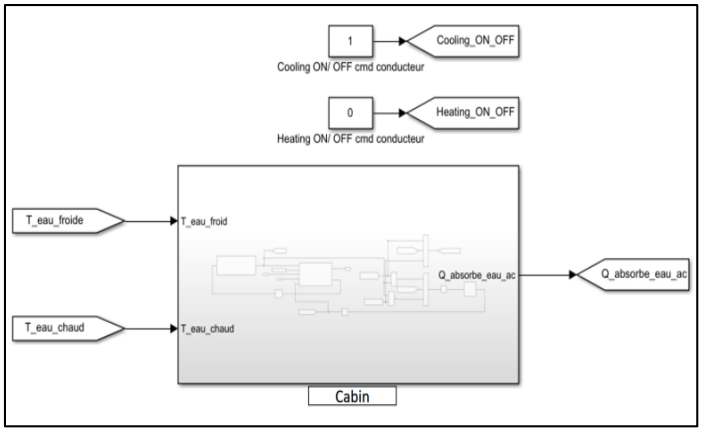

Figure 5. The Simulink block of the driver's cabin

Part 2: Radiator block of Powertrain components (PWT)

The radiator is essential to ensure that the hot or cold water leaving the PWT is reduced to room temperature before entering the tank. As in the radiator, we have the interaction of water with air, so the modeling is based on a thermal exchange between them.

For PWT cooling, cold water is circulated around the components before it is transferred to the radiator. The inlet temperature of the water is higher than the ambient temperature because the water absorbs heat from the PWT components. In the radiator, the water is reduced back to ambient (T water output) before returning to the tank (Figure 4).

Part 3: Cooler Block

The cold radiator is used to control the temperature of the passenger compartment. In the cold radiator there is an interaction between the cold/hot water and the air in the driver's cabin, for cooling or heating the driver's cabin. The modelling of the cold radiator was done in the same principle as the PWT radiator. A temperature controller was modelled to simulate the driver's choice of cabin temperature.

a. Driver's cabin: Model of an air tank with fixed volume/mass to simulate the driver's cab.

b. Cabin radiator: The model of the radiator is based on the same principle as the hot radiator explained above.

c. Controller: It is a controller which makes the request of water mass according to the difference of temperature between the cabin and the wished set point ('error' of temperature). This control is created with the help of a well-calibrated 1-D carto, to output the cold/hot water mass according to the temperature difference (or error) to cool/heat the air.

For the thermal management of the cabin simulation, the radiator is used to control the temperature of the passenger compartment.

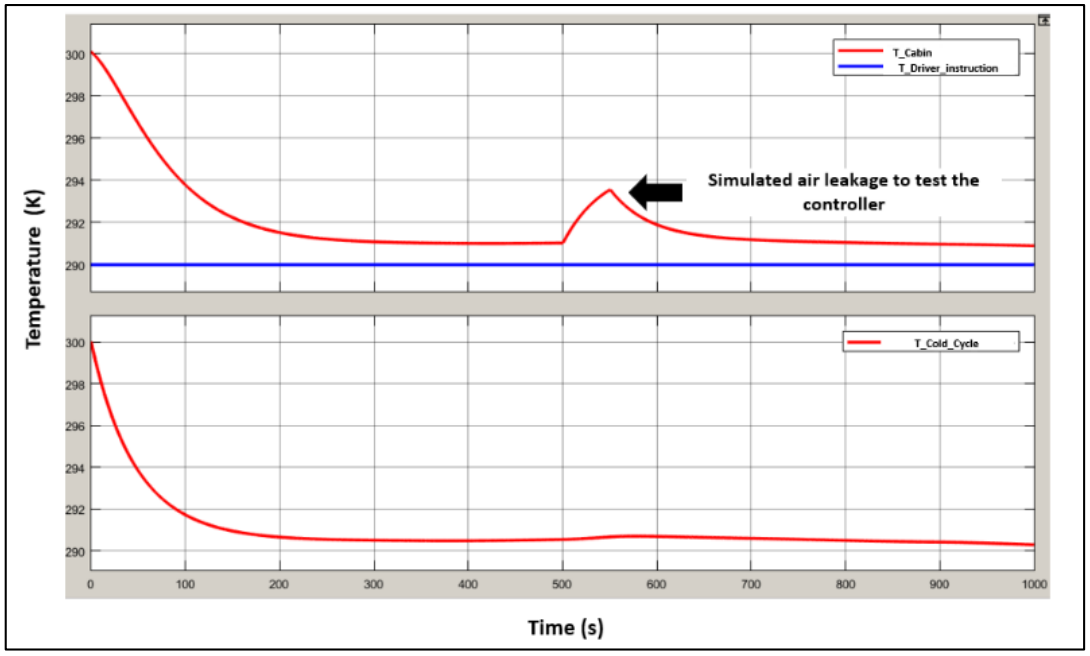

Figure 6. The simulation results of the cabin temperature and the air leakage

This model (Figure 5) takes account of an air tank with fixed volume and mass to simulate the driver's cab. This model radiator is based on the same principle of the Hot Radiator explained previously (see PWT radiator). The temperature set point given by the driver for heating/cooling is controlled within a defined temperature range. A controller for requesting the water mass based on the temperature difference between the cabin and the desired set point has been added to the model. This allows the temperature of the cabin to be regulated. The air temperature is calculated based on the weighted average:

- Total air mass = m_air.
- Air mass interacting with radiator = m_air_cycle.
- Air leakage mass = m_air_leakage.

Each air part is weighted with its temperature and the three parts were added to divide by total air mass to get the cabin temperature. The cabin temperature is reduced to close to the driver's desired setting. The small temperature difference is due to the efficiency of the radiator. It should also be noted that the possible cooling limit is related to the temperature of the cold water (Figure 6).

Part 4: PWT heat exchanger block

In this part, we performed the modelling for the heat exchange between hot water and PWT when the system needs to be heated. The hot water exchanger control of the PWT were analysed. The heat exchanger is activated or deactivated based on the need for heating or not for the PWT components. The control is based on continuing to heat the PWT components until all components reach room temperature (293 K). Then, when the heat exchanger is active, and one component needs more heating or reaches the temperature of 293 K before the other. In this case, the heating of all components is controlled separately. We calculate the heat absorbed by each PWT component battery, internal combustion engine and electric motor. And at the end, we calculate the decrease of the hot water temperature.

In addition, the modelling of energy absorbed by battery/ thermal or electric motor have been conducted. The heat exchange of all PWT components is modelled in the same direction as the temperature input corresponding to that component, T_battery / T_motor /T_elec. The heat exchange between the PWT components and the water is by convection:

$$Q = h \times A \times \Delta T \quad (19)$$

With:
A: the surface.
h: heat transfer coefficient.
ΔT: temperature variation.

Part 5: PWT cold exchanger block

This part is dedicated to the heat exchange model between cold water and PWT when the system needs to be cooled. When the system temperature is equal or higher than the ambient temperature and the PWT components start to work, there is a need to cool them to avoid a temperature increase that would exceed the limit. The objective is to ensure optimal operation of PWT components. As explained in the case of the hot exchanger, the operating principle for the cold exchanger is the same, but instead of heating, this exchanger is active when the PWT components need to be cooled. Therefore, the use of the hot or cold exchanger depends directly on the need of the PWT.

The activation of the cold exchanger is done when the temperature of all the PWT components are higher than 293 K. Therefore, if we start the simulation with an initial temperature of 293 K, the cold exchanger will be activated from the beginning. To control the cooling for each component based on its need, we have the same principle as for the heat exchanger. The water distribution is based on which component needs more energy to cool it.

Modelling of a cold exchanger of the PWT components was simulated. The modelling of the cold exchanger follows the same logic as for the hot exchanger. We calculate the heat dissipated by each component of the PWT (battery, internal combustion engine and electric motor). In general, the hybrid powertrain includes three components: the combustion engine, an electric motor powered by energy storage (such as a battery or fuel cell), and power electronics that produce heat and need to be cooled.

Part 6: PWT components model

The complete modelling of the battery, the electric motor and the combustion engine has been done by us (Figure 7). This part shows the outputs of these components necessary for the thermal management by the magnetocaloric system. The temperatures and the heat dissipated of these powertrain components during operation have been studied to perform a real time simulation. To test this magnetic cooling system model and the heat exchange between the water and the PWT car's drive train (to simulate heating or cooling), the PWT component model was added. The heat generated by the PWT components will be considered by the cooling system, which will adapt to either heat or cool, as needed. To calculate the temperature of each component, we use the heat generated by the component and add/decrease the heat added/dissipated by the hot/cold exchanger. Overall model is seen on Figure 8.

Total energy requirement (Q_{tot}) = Energy requirement for combustion engine (Q1) + Energy requirement for electric motor (Q2) + Energy requirement for battery (Q3)

Total water mass = m_water

Hot water mass for the heat engine = Q1 / Q_{tot} × m_water

Hot water mass for the electric motor = Q1 / Q_{tot} × m_water

Hot water mass for engine and battery = Q1 / Q_{tot} × m_water

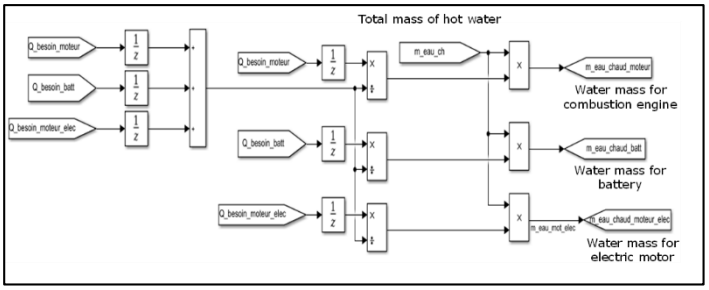

Figure 7. The simulation block of PWT components model

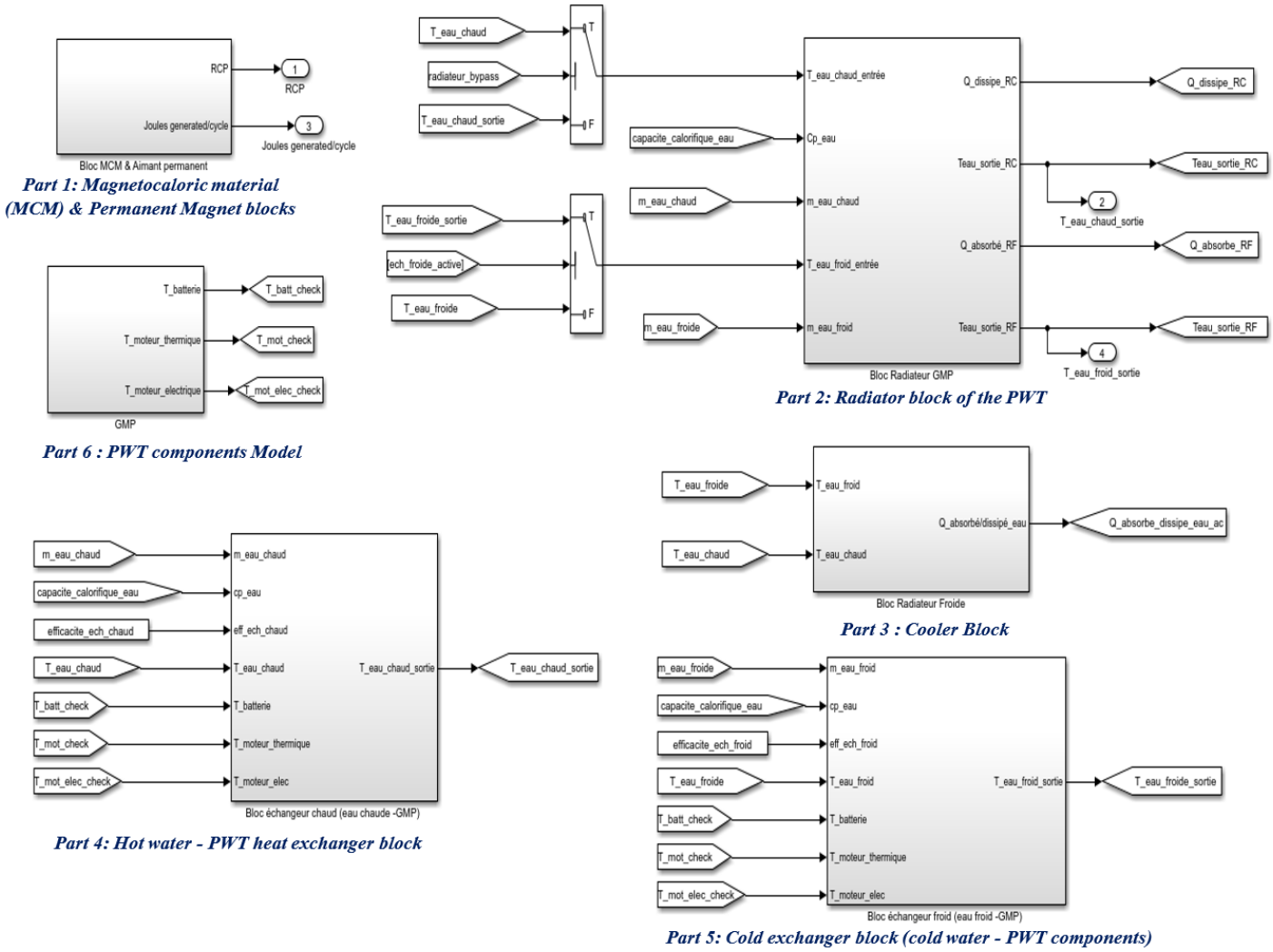

Figure 8. Interface of the global model of the magnetic cooling system and the powertrain components in Matlab-Simulink.

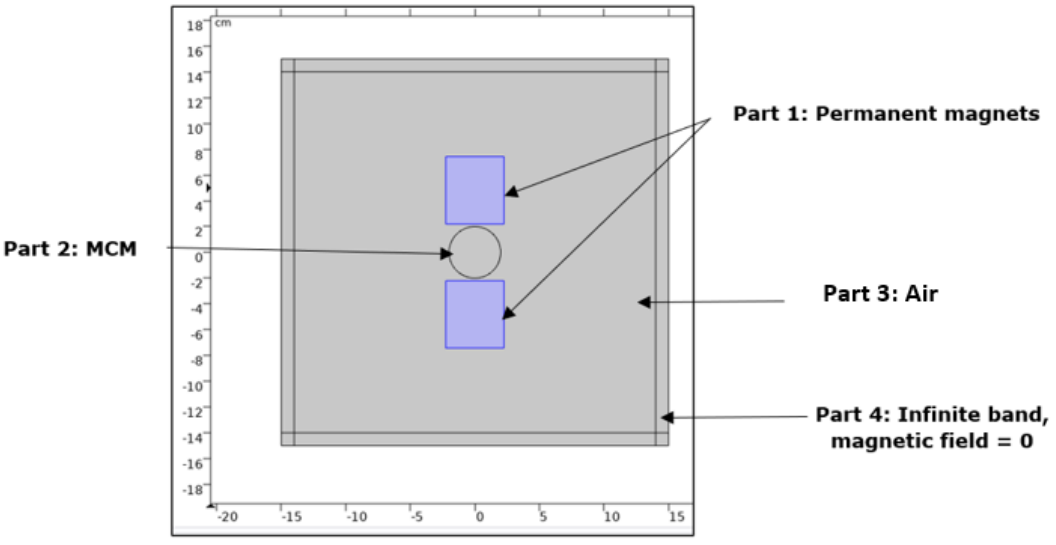

Figure 9. 2 Dimension COMSOL model of the MCM and permanent magnet.

4.2 COMSOL model

The COMSOL model enables to size and characterise the permanent magnet according to the magnetic field undergoes by the MCM block, as the distribution of the magnetic field lines changes according to the shape of the magnets.

The COMSOL model focuses on the study of the magnetic field generated by two parallel plate magnets in the magnetocaloric system.

There are four main parts to have the magnetic field simulated (Figure 9). For the part 1: Two magnetic blocks, whose properties have been defined to obtain the necessary magnetic field intensity. The part 2: the magnetocaloric material (MCM) block (circle of desired size), with the relative permeability defined to behave like Gadolinium (Gd). In the part 3: air of standard relative permeability

1 around the magnet and MCM. And finally, part 4: Infinite band around the borders to ensure zero magnetic field away from the magnets, to make the calculations converge.

The main parameters in the COMSOL model are defined. The relative air permeability was defined as 1. The square boundary was defined with a magnetic node point, i.e., the magnetic field at the edges is 0 T. The relative permeability of the MCM was defined as 100, based on several reviewed papers [19] and the magnetic property for permanent magnet blocks was assigned based on the method chosen for modelling. We tested three methodologies as mentioned below:

Method 1
Flux standard of remanent density = 1.4 T

Method 2
Magnetic flux density standard = 1.5 T (max 1.6 T)
Coercive field = 1500 kA/m
Magnetic energy density = 413 kJ/m

Method 3
Magnetization (Ms) = 1.6 T = 1276320 Amps/m

The third method based on the value of the magnetization, was chosen to make the simulation on COMSOL.

All other parameters have been fixed and the dimension only changes for permanent magnets. The distance between the MCM and the magnet has been fixed at 2 mm. The radius of the MCM has been fixed to 20 mm. The size of the permanent magnets varies based on two test cases, as explained below. So, to analyse all geometrical configurations, we studied two global use case based on the length of the permanent magnet (Table 1).

It should be noted that the mass and volume of the magnet have been set according to the operating characteristics of the magnetic cooling system. In each use case, we calculate the width and thickness according to the fixed length. The volume of a magnet plate is 188.3 cm^3 and the length of the plate are 9 cm and 8 cm: Table 2 summarises the characteristics of the permanent magnet and the magnetocaloric material.

$$\text{Width} \times \text{Thickness} = \text{Volume/Length} = 20.9\ cm^2 \quad (20)$$

Table 1. The use cases used for COMSOL simulation for the permanent magnet.

Use case 1 – Length = 9 cm	Use case 2 – Length = 8 cm
n combination of Width (cm) × Thickness (cm)	n combination of Width (cm) × Thickness (cm)
1st combination of 8 × 2.61	1st combination of 8×2.94
2nd combination of 7 × 2.98	2nd combination of 7×3.36
3rd combination of 6 × 3.48	3rd combination of 6×3.92
4th combination of 5.5 × 3.80	4th combination of 5.5×4.30
5th combination of 5 × 4.18	5th combination of 5×4.70
6th combination of 4.5 × 4.64	6th combination of 4.5×5.23

Table 2. Characteristics of the permanent magnet and the MCM.

Mass of the permanent magnet	2.9 kg
Mass density of Gadolinium	7700×10^{-6} kg/cm^3
Total volume of the permanent magnet	376.6 cm^3
Volume of a magnet plate	188.3 cm^3

In the two use cases, (9 cm and 8 cm long), we observe that the magnetic field strength increases by decreasing the width of the permanent magnet and increasing its thickness. (Figures 10 and 11).

After an analysis of the COMSOL study of permanent magnet and magnetocaloric material, the better combination is described in the Table 3 (use case 2). The value of the magnetic field intensity produced by the permanent magnet in this COMSOL simulation is about 1.48 T.

Table 3. Characteristics of the permanent magnet and the MCM.

Use case	Total mass (kg)	Length (cm)	Width (cm)	Thickness (cm)	Magnetic field max (Tesla)
Use Case 1	2.9	9	4.5	4.64	1.47
Use case 2	2.9	8	4.5	5.23	1.48

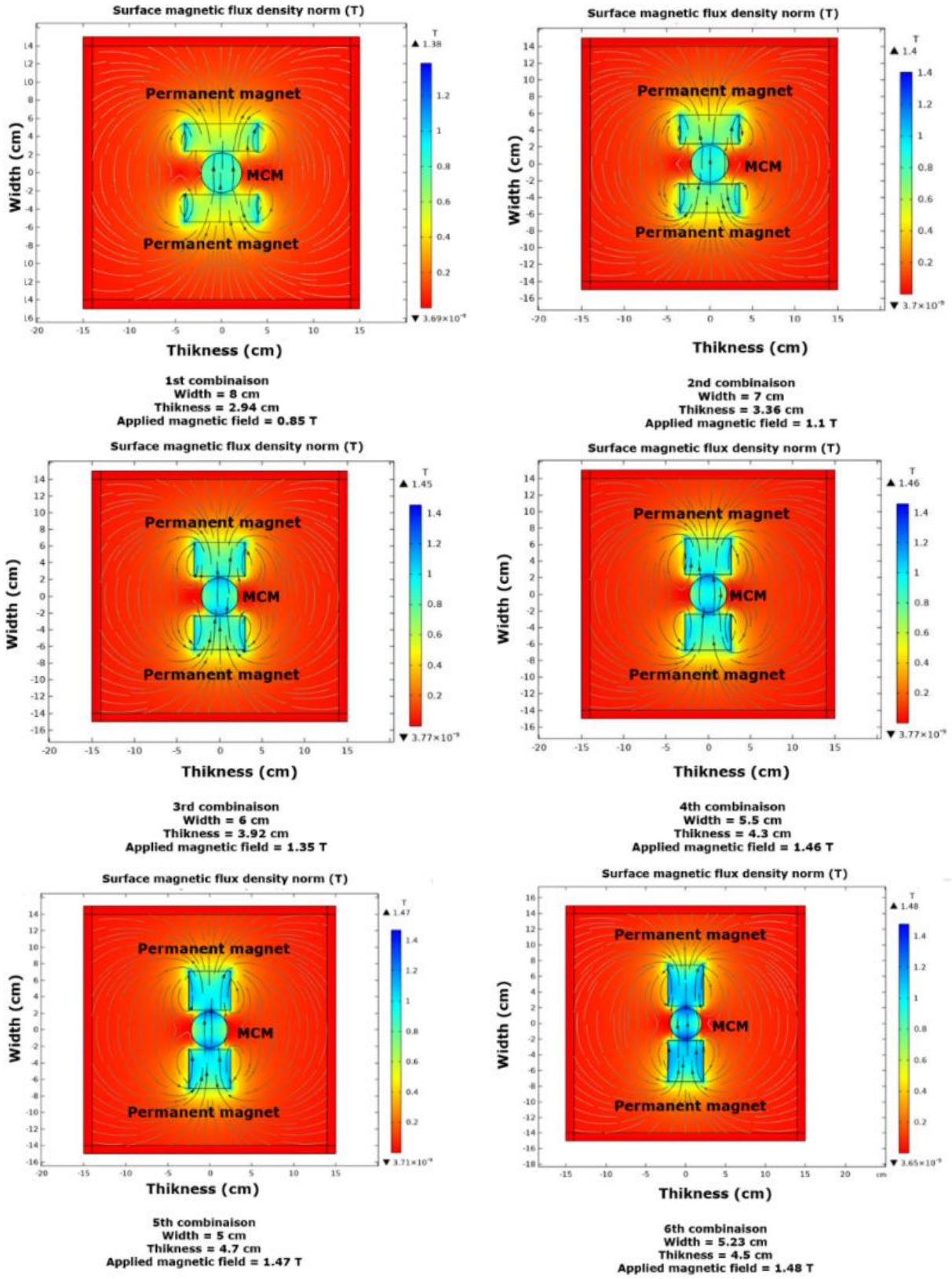

Figure 10. Evolution of the magnetic field intensity versus the width and thickness of the magnet (use case 1 - length 9 cm)

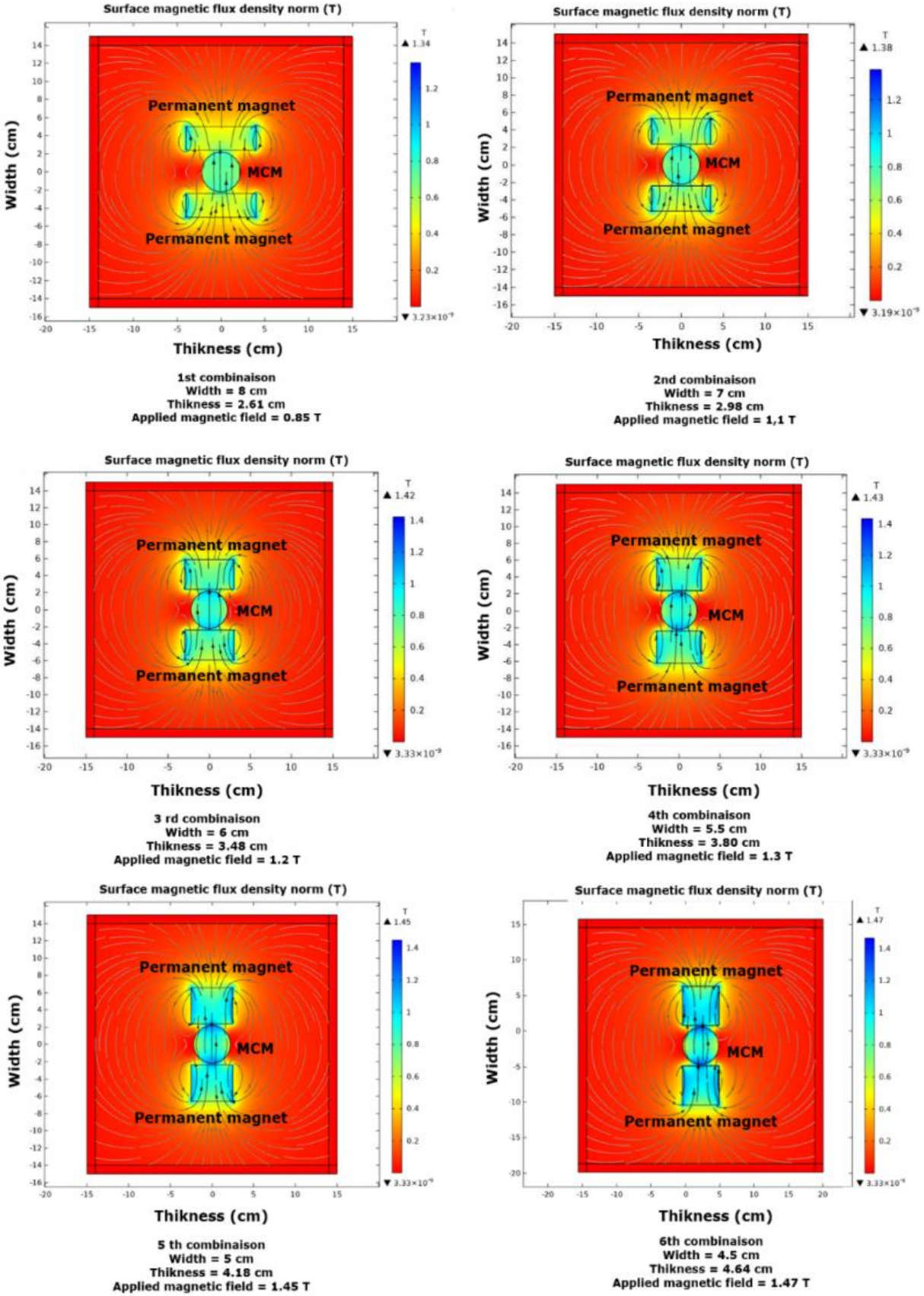

Figure 11. Evolution of the magnetic field intensity versus the width and thickness of the magnet (use case 2 - length 8 cm)

5. Conclusions

The objective of this paper was to study and understand the behavior of a magnetic cooling system at room temperature and to investigate and demonstrate the efficiency of this new technology.

To achieve this objective, a Matlab Simulink model was built of the permanent magnet, magnetocaloric material, the hybrid powertrain components as well as the water tanks, heat exchanger and radiators. In addition, to ensure the thermal management of the driver's cabin, a Simulink block has been added. This study was coupled with a two-dimensional model on the COMSOL software. This model allows to evaluate the behavior of the magnetocaloric material and the magnetic field intensity to improve the design and the energy consumption. The model developed in this study enables simulate a magnetic cooling system. The heat source which represents the magnetocaloric equation and approach is modelled based on the data obtained from experimental measurements.

Acknowledgment

This work was supported by Capgemini engineering-France (Innovative and Intelligent Powertrain Research & Innovation Department). The authors would like to thank the other members of the team, Fatima Haidar, Chayma Mohsni, Racha Bayzou and Thierry Bertau. The authors would also like to thank the interns of the iPowertrain project.

Nomenclature

MCE	magnetocaloric effect
CT	curie transition
H	magnetic field (T)
T	temperature (K)
P	pressure
G	Gibbs free energy
U	internal energy of the system
V	Volume (m^3)
M	magnetization
S	entropy
μ_0	magnetic permeability of the vacuum
RCP	relative cooling power (J/kg)
Q	energy (J)
PWT	powertrain
m_air	total air mass (kg)
m_air_cycle	air mass interacting with radiator (kg)
m_air_leakage	air leakage mass (kg)
A	Surface (m^2)
h	heat transfer coefficient (W/(m.K))
m_water	total water mass (kg)
MCM	magnetocaloric material
T_ini	initial temperature of PWT/ tank (K)

Conflict of Interest Statement

All authors have given approval to the final version of the manuscript. The authors declare that there is no conflict of interest in the study.

CRediT Author Statement

Mohand-Ouyahia Bousseksou: Writing- review & editing, supervision, project leader, methodology & software, **Kamal Nouri:** Writing original draft & editing, **Thomas Bartoli:** Formal analysis, **Wassim Bouzidi:** Formal analysis **Lotfi Bessais:** Review & editing.

References

1. Torregrosa-Jaime, B., Corberán, J. M., Vasile, C., Muller, C., & Risser, M. (2014). Sizing of a reversible magnetic heat pump for the automotive industry. International Journal of Refrigeration, 37, 156-164. https://doi.org/10.1016/j.ijrefrig.2013.06.018
2. Achkar, G. E., B. Liu, & R. Bennacer. (2019). Numerical study on the thermohydraulic performance of a reciprocating room temperature active magnetic regenerator. E3S Web Conf, 128, 07001. https://doi.org/10.1051/e3sconf/201912807001
3. Broughton, J., Vanessa Smet, Rao R. Tummala, & Yogendra K. Joshi. (2018). Review of Thermal Packaging Technologies for Automotive Power Electronics for Traction Purpose. Journal of Electron Packaging, 140, 040801. https://doi.org/10.1115/1.4040828
4. C Vasile, & C Müller. (2006). Innovative design of a magnetocaloric system. International Journal of Refrigeration, 29, 1318-1326. https://doi.org/10.1016/j.ijrefrig.2006.07.016
5. T. Lehy et G. Willems. (1976). Population Kinetics of Antral Gastrin Cells in the Mouse. Gastroenterology, 71, 614-619. https://doi.org/10.1016/S0016-5085(76)80552-5
6. Lionte, S., Carmen Vasile, & Monica Siroux . (2014). La réfrigération magnétique : technologie innovante. COFRET'14- PF3-041, 14. https://doi:10.13140/2.1.3946.5767
7. Lee, S. J., J. M. Kenkel, V. K. Pecharsky, & D. C. Jiles . (2002). Permanent magnet array for the magnetic refrigerator. Journal of Applied Physics, 91, 8894. http://doi.org/10.1063/1.1451906
8. Okamura, T., Kazuhiko Yamada, Naoki Hirano, Naoki Hirano, & Shigeo Naga. (2006). Performance of a room-temperature rotary magnetic refrigerator. International Journal of Refrigeration, 29, 1327-1331. http://10.1016/j.ijrefrig.2006.07.020.
9. Nouri, K., M. Saidi, L. Bessais, & M. Jemmali. (2021). Structural, magnetic and magnetocaloric study of Sm 2 Fe 17−x Ni x (x = 0, 0.25, 0.35 and 0.5) compounds. Applied Physics, 127, 442. https://doi.org/10.1007/s00339-021-04546-1
10. Nouri, K., T. Bartoli, A. Chrobak, J. Moscovici , & L. Bessais . (2018). Magnetism and Hyperfine Parameters in Iron Rich Gd2Fe17-xSix Intermetallics. Journal of Electronic Materials, 47, 3836–3846. https://doi.org/10.1007/s11664-018-6256-z
11. Bouzidi, W., Bartoli, T., Sedek, R., Bouzidi, A., Moscovici, J., & Bessais, L. (2021). Low-field magnetocaloric effect of NdFe _ 11 Ti NdFe 11 Ti and SmFe _ 10 V _ 2 SmFe 10 V 2 compounds. Journal of Materials Science: Materials in Electronics, 32, 10579-10586. https://doi.org/10.1007/s10854-021-05713-z
12. Pecharsky, V. K., & K. A. Gschneidner, Jr. (1997). Giant Magnetocaloric Effect in Gd5(Si2Ge2). Physical Review Letters, 78, 4494-4497. https://doi.org/10.1103/PhysRevLett.78.4494
13. WadaY, H., & Y. Tanabe. (2001). Giant magnetocaloric effect of MnAs1−xSbx. 79, 3302-3304. https://doi.org/10.1063/1.1419048
14. Hu, F.-x., Bao-gen Shen, Ji-rong Sun, Zhao-hua Cheng, Guang-hui Rao, & Xi-xiang Zhang. (2001). Influence of negative lattice expansion and

metamagnetic transition on magnetic entropy change in the compound LaFe11.4Si1.6. Applied Physics Letters, 78, 3675-3677. https://doi.org/10.1063/1.1375836

15. Tegus, O., E. Brück, K H J. Buschow, & F R de Boer. (2002). Transition-metal-based magnetic refrigerants for room-temperature applications. 415, 150–152. https://doi.org/10.1038/415150a
16. Zou, J. D., H. Wada, B. G. Shen, J. R. Sun, & W. Li. (2008). Giant magnetocaloric effect and soft-mode magneto-structural phase transition in MnAs. Europhysics Letters, 81, 47002. https://doi:10.1209/0295-5075/81/47002
17. Duchoň, F., Andrej Babinec , Martin Kajan, Peter Beňo , Martin Florek, Tomáš Fico, & Ladislav Jurišica. (2014). Path Planning with Modified a Star Algorithm for a Mobile Robot. Procedia Engineering, 96, 59-69. https://doi.org/10.1016/j.proeng.2014.12.098
18. Jaballah, H., Kamel Nouri, Najeh Mliki, Lotfi Bessais, & Mosbah Jemmali. (2022). Investigation of Magnetic Entropy Change in Intermetallic Compounds SmNi3–xFex Based on Maxwell Relation and Phenomenological Model. Crystals, 12, 481. https://doi.org/10.3390/cryst12040481
19. Fraga, G. L., Paulo Pureur, & Lisandro Pavie Cardoso. (2010). Impedance and initial magnetic permeability of gadolinium. Journal of Applied Physics, 107, 053909. https://doi.org/10.1063/1.3288696